



# Pressure-induced phase transitions for goethite investigated by Raman spectroscopy and electrical conductivity

Kaixiang Liu, Lidong Dai, Heping Li, Haiying Hu, Yukai Zhuang, Linfei Yang, Chang Pu & Meiling Hong


To cite this article: Kaixiang Liu, Lidong Dai, Heping Li, Haiying Hu, Yukai Zhuang, Linfei Yang, Chang Pu & Meiling Hong (2019): Pressure-induced phase transitions for goethite investigated by Raman spectroscopy and electrical conductivity, High Pressure Research

To link to this article: <https://doi.org/10.1080/08957959.2019.1572751>



Published online: 29 Jan 2019.



Submit your article to this journal 



View Crossmark data 



## Pressure-induced phase transitions for goethite investigated by Raman spectroscopy and electrical conductivity

Kaixiang Liu<sup>a,b</sup>, Lidong Dai<sup>a</sup>, Heping Li<sup>a</sup>, Haiying Hu<sup>a</sup>, Yukai Zhuang<sup>a,b</sup>, Linfei Yang<sup>a,b</sup>, Chang Pu<sup>a,b</sup> and Meiling Hong<sup>a,b</sup>

<sup>a</sup>Key Laboratory of High-Temperature and High-Pressure Study of the Earth's Interior, Institute of Geochemistry, Chinese Academy of Sciences, Guiyang, Guizhou, People's Republic of China; <sup>b</sup>University of Chinese Academy of Sciences, Beijing, People's Republic of China

### ABSTRACT

We reported two pressure-induced phase transitions of goethite up to ~35 GPa using a diamond anvil cell in conjunction with impedance spectroscopy, Raman spectra at room temperature. The first pressure-induced phase transition at ~7.0 GPa is manifested in noticeable changes in six Raman-active modes, two obvious splitting phenomena for the modes and the variations in the slope of conductivity. The second phase transition at ~20 GPa was characterized by an obviously drop in electrical conductivity and the noticeable changes in the Raman-active modes. The variations in activation energy with increasing pressure were also discussed to reveal the electrical properties of goethite at high pressure.

### ARTICLE HISTORY



Received 13 July 2018  
Accepted 21 December 2018

### KEYWORDS

Goethite; high pressure; Raman spectroscopy; electrical conductivity; phase transition

## Introduction

Goethite ( $\alpha$ -FeOOH) that belongs to the group of XOOH minerals ( $X = \text{Fe, Al, Mn, Co, and Cr}$ ) is a primary component of rust at the Earth's surface and is one of the most widespread iron oxy-hydroxides in terrestrial soils, sediments, and ore deposits [1]. Except for goethite, three typical iron oxy-hydroxides contain akaganeite ( $\beta$ ), lepidocrocite ( $\gamma$ ) and the high pressure phase ( $\epsilon$ ). At ambient pressure, goethite crystallizes in a complex orthorhombic structure (space group  $Pbnm$ ,  $Z = 4$ ), which can be described as a slightly hexagonally distorting close to the packing of oxygen on iron atoms occupying two-third of the octahedral sites [2]. The  $\text{FeO}_6$  octahedra are linked by sharing edges and vertices to form infinite  $2 \times 1$  channels parallel to the  $b$  axis with hydrogen atoms inside the channels. With three short [1.933(3), 1.962(2) Å] and three long [2.107(3) Å] Fe–O bonds, the  $\text{FeO}_6$  octahedra become highly distorted. The oxygen O1 ligands in the longer Fe–O bonds designated as Fe–O1 correspond to the covalently bound oxygen of the hydroxyl, while other oxygen O2 ligands in the short Fe–O bonds are weakly bound to hydrogen in the nearest neighbor hydroxyl [2].

**CONTACT** Lidong Dai  dailidong@vip.gyig.ac.cn  Key Laboratory of High-Temperature and High-Pressure Study of the Earth's Interior, Institute of Geochemistry, Chinese Academy of Sciences, Guiyang, Guizhou 550081, People's Republic of China

Hydrous minerals play an important role in transporting water into Earth's interior and thereby have one crucial influence on the geophysical and geochemical processes [3–6]. As the most stable and common hydrous minerals among the iron oxy-hydroxides at ambient conditions, goethite has attracted a lot of wide interests in the field of high pressure mineral physics and material science [7–12]. Previous reports about goethite at high pressure mainly focus on the structural parameters and phase transitions on the basis of X-ray diffraction (XRD), infrared (IR) spectra and first theoretical calculations. Williams and Guenther [7] found that a double peak turns into a single peak on the infrared spectroscopy of goethite at 9.8 GPa. Nagai et al. [8] observed no evidences for pressure-induced phase transitions for goethite up to 24 GPa at room temperature by means of XRD and Gleason et al. [9] obtained the same result at the pressure range of 0–29 GPa. While the  $\alpha$  to  $\varepsilon$  high pressure phase transition was detected at the pressure range of 5.9 and 7 GPa by first theoretical calculations [10]. Suzuki et al. [12] observed the change in compression behavior on axes between 4 and 5 GPa. Although measurements of high pressure electrical transport and Raman spectroscopy are important for detecting the subtle changes that occur during the pressure-induced phase transition, the data about conductivity and Raman spectroscopy are still infrequent. To the best of our knowledge, only one high pressure electrical resistivity experiment has been reported in a wide pressure range up to  $\sim 72$  GPa for goethite [11]. As for the Raman spectroscopy measurement, only one report about goethite above  $\sim 30$  GPa without any sufficient discussion [11]. In view of the open questions and controversies in the phase transitions of goethite at high pressure, further systematic investigation of the electrical properties and Raman spectroscopy at high pressure is required to determine whether pressure-induced phase transition occurs for goethite.

In the present study, we reported two pressure-induced phase transitions for goethite up to 35.0 GPa at room temperature using a diamond anvil cell (DAC) in conjunction with ac impedance spectroscopy and Raman spectroscopy. Furthermore, those two correspondent phase transitions for goethite were discussed in detail at high pressure.

## Experimental methods

The 99.999% goethite ( $\alpha$ -FeOOH) powder was commercially purchased from Alfa-Aesar. High pressure Raman spectroscopy experiments were performed using a DAC with a 300  $\mu\text{m}$  anvil culet. A ruby single crystal with a grain size of  $\sim 5$   $\mu\text{m}$  was used for pressure calibration on the basis of the wavenumber shift of the fluorescence band of  $\text{Cr}^{3+}$  ions. Helium was used as the pressure medium to provide a hydrostatic condition, and no pressure medium was used for the nonhydrostatic condition. Raman spectra were collected using a Raman spectrometer (Invia, Renishaw) equipped with a CCD camera (Olympus) and a confocal microscope (TCS SP8, Leica). The excitation laser powers were typically 20 mW for the Raman spectra and 0.5–40  $\mu\text{W}$  for fluorescence. As for high temperature and high pressure Raman scattering experiments, the sample cell load was enhanced to a predesigned pressure, and then the temperature was gradually raised up to 350°C by intervals of 50°C. Spectra were taken for the backscattering geometry using an argon ion laser (Spectra physics; 514.5 nm and power  $< 1$  mW) in the range of 150–900  $\text{cm}^{-1}$  with a spectral resolution of 1.0  $\text{cm}^{-1}$ . To avoid pressure oscillation, the DAC pressure equilibration time was 1 h at each pressure point before the spectral acquisition.

In order to determine the positions of the Raman modes, Raman spectra were fitted by a Lorenz-type function using PeakFit software. And the fitted error bar is also fully considered.

High pressure electrical conductivity experiments were conducted in a DAC with a 300  $\mu\text{m}$  anvil culet. The sample was crushed into a powder ( $\sim 20\ \mu\text{m}$ ). A T-301 stainless steel gasket was pre-indented to a thickness of  $\sim 60\ \mu\text{m}$  and a 180- $\mu\text{m}$  hole was drilled with a laser. A 100- $\mu\text{m}$  hole was drilled as an insulating sample chamber, after a mixture of boron nitride powder and epoxy compressed into the hole. [Figure 1](#) shows the cross-sectional assembly of the designed DAC used in this study. AC impedance spectroscopy was performed with the Solartron-1260 and Solartron-1296 impedance spectroscopy analyzers with the frequency range of  $10^{-1}$ – $10^7$  Hz. A plate electrode was integrated between two symmetric diamond anvils [13]. Detailed descriptions of the high pressure equipment and experimental procedures can be found elsewhere [14–17].

## Results and discussion

Raman spectroscopy is an effective probe for detecting phase transitions at high pressure [17]. [Figure 2](#) shows the Raman spectra of goethite at room temperature up to  $\sim 30.0$  GPa. Below 7.0 GPa, six typical Raman vibration modes are observed, which are attributed as follows: the peaks at 243 and 676  $\text{cm}^{-1}$  corresponded to symmetric Fe–O stretching vibrations, respectively; the peak at 299  $\text{cm}^{-1}$  corresponded to symmetric Fe–OH bending vibration; the peak at 388  $\text{cm}^{-1}$  corresponded to symmetric Fe–O–Fe/OH stretching vibration; and for the peaks at 484 and 551  $\text{cm}^{-1}$  corresponded to antisymmetric Fe–OH stretching vibrations [18]. All these obtained modes are consistent with previously reported experimental results [19, 20]. The pressure dependences of Raman modes for goethite and the obtained fitting results are displayed in [Figure 2](#) and [Table 1](#), respectively.

In the progress of compression, all of the observed Raman modes could be divided into three intervals: below 7.0 GPa, between 7.0 and 20.0 GPa and above  $\sim 20.0$  GPa. Under a nonhydrostatic condition, we obtained six positive  $\partial\omega/\partial P$  values ( $\omega$  and  $P$  are the assumed Raman shift and pressure, respectively) from 0.43–1.20  $\text{cm}^{-1}\ \text{GPa}^{-1}$  for all

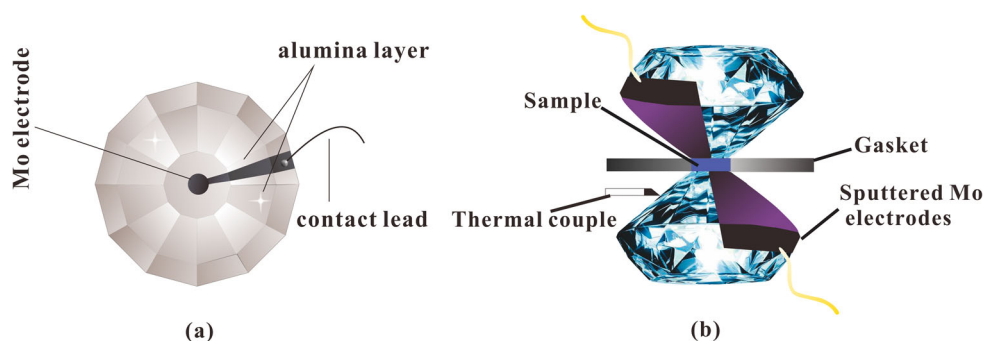


**Figure 1.** Experimental assembly for electrical conductivity measurement for goethite. (a) Configuration of plate electrodes integrated between two symmetric diamond anvils. (b) Cross section of the DAC used for impedance spectroscopy measurement at high pressure.

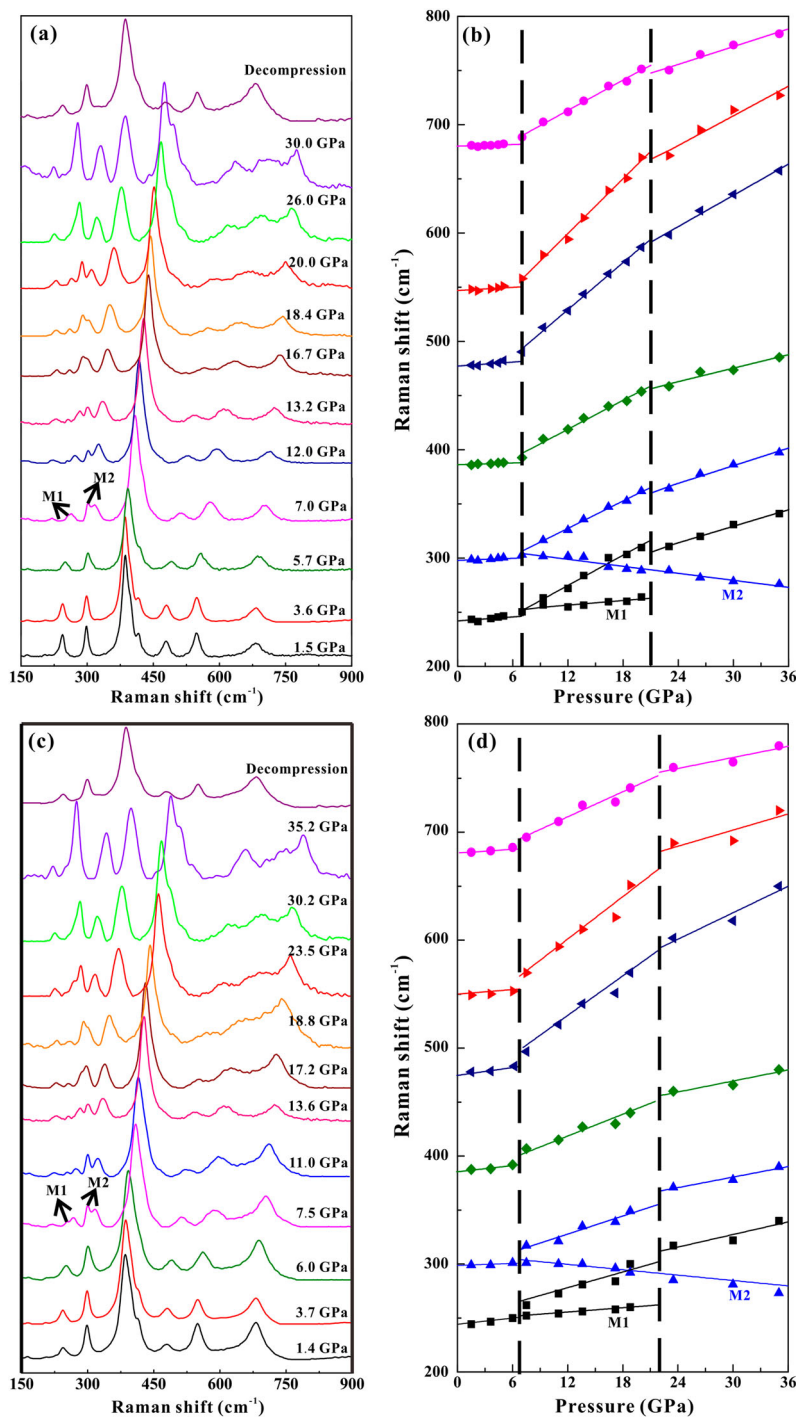


**Figure 2.** Raman spectroscopic results of at high pressure. (a), (c) Raman spectra at each representative pressure point ( $\lambda = 514$  nm and  $T = 300$  K). (b), (d) Raman mode frequency evolution against pressure for goethite in nonhydrostatic and hydrostatic conditions, respectively. Two new Raman modes appeared at  $\sim 7.0$  GPa (denoted as M1 and M2). Errors in both frequency and pressure are within the size of the symbol.

**Table 1.** Pressure dependence of the Raman shift for goethite under nonhydrostatic and hydrostatic conditions.

Pressure condition	$\omega(P)$ ( $\text{cm}^{-1}$ )	$\partial\omega/\partial P$ ( $\text{cm}^{-1} \text{GPa}^{-1}$ ) < 7.0 (GPa)	$\partial\omega/\partial P$ ( $\text{cm}^{-1} \text{GPa}^{-1}$ ) > 7.0 (GPa)	$\partial\omega/\partial P$ ( $\text{cm}^{-1} \text{GPa}^{-1}$ ) > 20.0 (GPa)
Nonhydrostatic	243	0.49	4.66	2.73
	257	–	0.70	–
	299	0.62	4.22	2.73
	302	–	–1.10	–1.10
	388	0.53	4.46	2.10
	484	1.20	7.23	4.84
	551	0.94	8.44	4.50
	676	0.43	4.66	2.04
Hydrostatic	243	0.65	2.30	1.93
	257	–	0.66	–
	299	0.45	2.92	1.62
	302	–	–0.73	–0.73
	388	0.78	3.84	1.70
	484	1.50	7.60	4.09
	551	0.69	7.08	3.10
	676	0.78	4.03	2.01

Note: The peaks at 257 and 302  $\text{cm}^{-1}$  are the new Raman modes appeared at  $\sim 7.0$  GPa.

these six typical Raman modes below 7.0 GPa. Between 7.0 and 20.0 GPa, we obtained seven positive  $\partial\omega/\partial P$  values from 0.70 to 8.44  $\text{cm}^{-1} \text{GPa}^{-1}$ , and one negative  $\partial\omega/\partial P$  value of  $-1.10 \text{ cm}^{-1} \text{GPa}^{-1}$ . Above 20.0 GPa, we obtained six positive  $\partial\omega/\partial P$  values from 2.04 to 4.84  $\text{cm}^{-1} \text{GPa}^{-1}$  and one negative  $\partial\omega/\partial P$  value of  $-1.10 \text{ cm}^{-1} \text{GPa}^{-1}$ . Under a hydrostatic condition, six positive  $\partial\omega/\partial P$  values from 0.45 to 1.50  $\text{cm}^{-1} \text{GPa}^{-1}$  for all these six typical Raman modes are obtained below 7.0 GPa. Except one negative  $\partial\omega/\partial P$  value of  $-0.73 \text{ cm}^{-1} \text{GPa}^{-1}$  for M2 mode, seven positive  $\partial\omega/\partial P$  values from 0.66 to 7.60  $\text{cm}^{-1} \text{GPa}^{-1}$  are obtained between 7.0 and 20.0 GPa. Six positive  $\partial\omega/\partial P$  values from 1.62 to 4.09  $\text{cm}^{-1} \text{GPa}^{-1}$  and one negative  $\partial\omega/\partial P$  value of  $-1.10 \text{ cm}^{-1} \text{GPa}^{-1}$  are obtained above 20.0 GPa. It's well-known that the shortening of the bond distance would cause a Raman frequency increase, while the enlargement of the equilibrium angle would lead to a decrease in Raman frequency [20]. All of the positive  $\partial\omega/\partial P$  values indicate pressure-induced contraction for the distance of atoms in goethite in the progress of compression, while the negative  $\partial\omega/\partial P$  values of mode at 302  $\text{cm}^{-1}$  (M2) may indicate the enlargement of the bond angle in goethite in the progress of compression.

At  $\sim 7.0$  GPa, we detected two obvious splitting phenomena for the modes at 243 and 299  $\text{cm}^{-1}$  accompanies with four new separate peaks at 257  $\text{cm}^{-1}$  (M1), 263, 302  $\text{cm}^{-1}$  (M2) and 316  $\text{cm}^{-1}$ , respectively. With increasing pressure, we observed the vanishing of M1 mode above 20 GPa. And the Raman spectroscopy in our measurements at 30.0 GPa has a good consistence with previous results reported by [11]. As for the pressure dependence of Raman modes, two obvious discontinuities at 7.0 and 20.0 GPa were discovered. Considering the new Raman modes and the discontinuities in pressure dependence of Raman modes, the compound may have undergone new pressure-induced phase transitions at 7.0 and 20.0 GPa.

In fact, Nagai et al. [8] report a kink at  $\sim 10$ –11 GPa in the volume versus pressure dependence accompanied by a discontinuous broadening of diffraction peaks. Similar features were observed also by Gleason et al. [9] above  $\sim 8$  GPa. But they attributed the variations on volumes and lattice parameters to the solidification of the 4:1 methanol:ethanol

pressure medium introducing non-hydrostaticity. In order to avoid the influence of the 4:1 methanol:ethanol pressure medium, we measured the Raman spectroscopy under hydrostaticity condition with pressure medium of Helium. As shown in Figure 2(c), (d) and Table 1, both the Raman spectrum and the Raman shift of goethite under hydrostatic condition at high pressure show a strong evidence for pressure-induced phase transitions of goethite at  $\sim 7.0$  and  $\sim 20.0$  GPa that two obvious splitting phenomena and the noticeable changes of all Raman-active modes. Although previous high pressure XRD results were associated with solidification of the pressure medium, they may be overlapped by the phase transition. Recently, Suzuki et al. [12] observed the discontinuous change of the parameter axial ratio of goethite between 4 and 5 GPa by X-ray diffraction with the pressure medium of NaCl. Besides, there exist many discrepancies according to the previous results on the bulk modulus for goethite, which possibly denotes a pressure-induced phase transition of sample. For example, 85.9 GPa by Suzuki et al. [12] at the pressure range of 0–7, 120 GPa by Xu et al. [11] at the pressure range of 0–16, 140.3 GPa by Gleason et al. [9] at the pressure range of 0–29 GPa. This higher bulk modulus value (140.3 GPa) for goethite by Gleason et al. [9] even exceeds the isostructural diaspora (134.4 GPa), which has a substantially smaller unit cell volume with a relatively higher bulk modulus than goethite [21]. And as for the high pressure ( $\epsilon$ ) phase, the bulk moduli becomes higher than  $\alpha$ -FeOOH [10]. In the light of the appearance of new Raman modes at  $\sim 7.0$  GPa and this variation in the experimental bulk modulus with the pressure interval, we believe goethite suffers a phase transition from  $\alpha$ -FeOOH to high pressure ( $\epsilon$ ) phase at  $\sim 7.0$  GPa.

To further verify the high pressure phase of goethite is the epsilon phase, a series of high temperature Raman spectroscopy measurements have been conducted at high

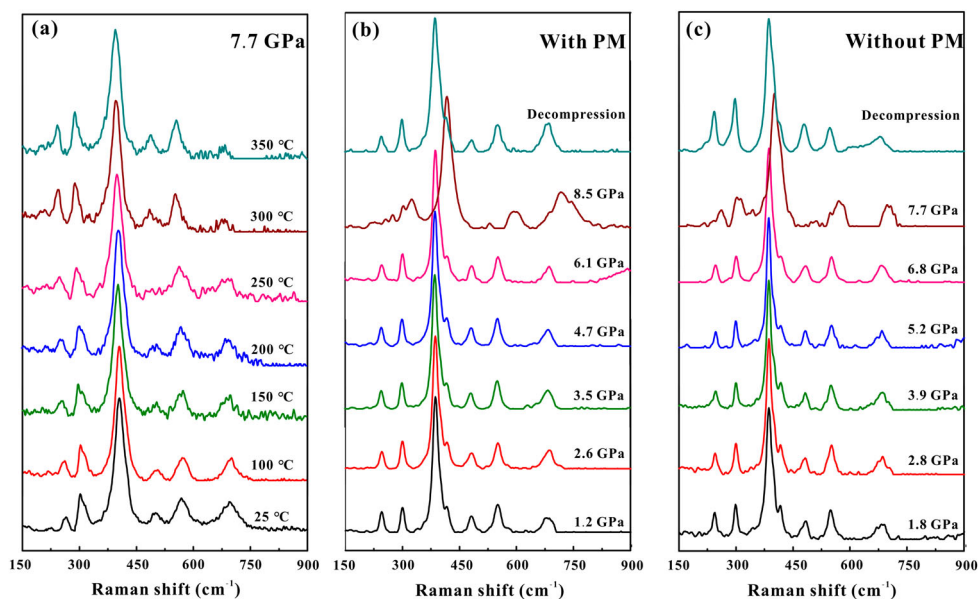


**Figure 3.** (a) Raman spectra at different temperatures with pressure of  $\sim 7.7$  GPa. ( $\lambda = 514$  nm). (b) and (c) Raman spectra at each representative pressure point with a narrow pressure range of 1.2–8.5 GPa at different hydrostatic conditions.

temperature (100–350°C) and high pressure (7.7 GPa). Figure 3 shows the representative Raman spectra of goethite under conditions of the temperature range of 25–350°C and pressure of  $\sim 7.7$  GPa. In consideration of the pressure–temperature diagram of the FeOOH system reported by Wiethoff et al. [22], goethite suffers a phase transition from  $\alpha$  to  $\varepsilon$  phases at the pressure above 7.1 GPa and temperature above 310°C. In the present study, the Raman modes tend to move towards lower frequencies with increasing temperature at the pressure of 7.7 GPa without any new Raman mode. Our obtained high temperature and high pressure Raman spectroscopy results do not provide a clear evidence for phase transitions above 300°C. Thus we believe goethite suffers a phase transition from  $\alpha$ -FeOOH to high pressure ( $\varepsilon$ ) phase at  $\sim 7.0$  GPa. As for whether the high pressure phase of goethite would be quenched, it is still remained controversial. Wiethoff et al. [22] and Suzuki [23] obtained the quenchable epsilon phase of FeOOH at the pressure above 7.1 GPa and the temperature above 310°C. While Gleason et al. [9] obtain the non-quenchable epsilon phase of FeOOH at the pressure above  $\sim 6.0$  GPa and the temperature above 300°C. A reversible phenomenon of goethite upon decompression from  $\sim 54.0$  GPa was also observed by Xu et al. [11]. Figure 3(b, c) shows the Raman spectra at each representative pressure point with a narrow pressure range of 0–8.5 GPa at different hydrostatic conditions. As shown in Figure 3(b, c), all the obtained Raman spectra show a dramatic variation at the pressure of  $\sim 7$  GPa, which accompanied by a reversible characteristic Raman peak during decompression up to room pressure. Our experimental results further demonstrate that the pressure-induced phase transition at  $\sim 7$  GPa of goethite is reversible regardless of the experimental pressure range and the hydrostatic conditions. In other words, the high pressure epsilon phase of goethite is non-quenchable, which is in good agreement with the previously obtained results by Gleason et al. [9] and Xu et al. [11]. Besides, the decompressed Raman spectra upon from 35.2 GPa of goethite is also recovered to its original state (Figure 2), which indicates a reversible phase transition.

As we known, it is one effective method that we can extrapolate the type of phase transition by virtue of those of characteristic parameter variations in the synchrotron X-ray diffraction upon compression, such as the unit cell volume, the crystalline lattice parameters, the axial ratio, the bond length et al. [24,25]. In one hand, the occurrence of the pressure-induced first-order phase transition was characterized by the unit cell volume collapsing at high pressure condition. On the other hand, the pressure-induced second-order isostructural phase transition was ordinarily confirmed by these of obvious discontinuities in the axial ratio and the bond length along with a continuous unit cell volume and the crystalline lattice parameter variation before and after phase transition. Some observations on the synchrotron X-ray diffraction for goethite have been conducted by Xu et al. at the wide pressure range from 0 to 57 GPa using the DAC [11]. Xu et al. found one obvious discontinuity in the O1–O2 bond length with the continuous crystalline lattice parameter at the pressure of 20 GPa. And therefore, in the present work, owing to a discontinuity in the pressure dependence of Raman modes without any appearance of the new peak, our observed pressure-induced phase transition belongs to a second-order isostructural phase transition at  $\sim 20.0$  GPa.

Structural phase transition is often accompanied by the change of electrical properties at the same time. To further verify the phase transition in goethite, pressure-induced electrical conductivity measurements were carried out up to  $\sim 35.0$  GPa at atmospheric



temperature. The representative Nyquist plots of the impedance spectroscopy of goethite under high pressures were shown in Figure 4(a)–(c) in the pressure range of 1.6–35.0 GPa. The plots were fitted by ZView software (equivalent circuit method). The impedance spectra are well separated into two parts: a semicircular arc in the higher-frequency region corresponds to the grain interior contribution and an oblique line at a lower frequency corresponds to the grain boundary contribution. In the present study, particular attention was paid to the variation of grain interior contribution reflected in phase transitions.

The electrical conductivity of the parallel plate electrode can be obtained as follows:

$$\sigma_b = \frac{1}{R_b} \left( \frac{l}{A} \right), \quad (1)$$

where  $A$  and  $l$  denote the electrode area and the distance between the two electrodes, respectively. Figure 4(d) shows the pressure-dependent logarithm of the electrical conductivity of goethite in the process of compression at room temperature. The electrical conductivity of goethite increases gradually from ambient pressure to 20.5 GPa, and shows a dramatic difference trends around 6.8 GPa. The slope of pressure versus conductivity decreases with increasing pressure below 6.8 GPa, while the slope shows an increased

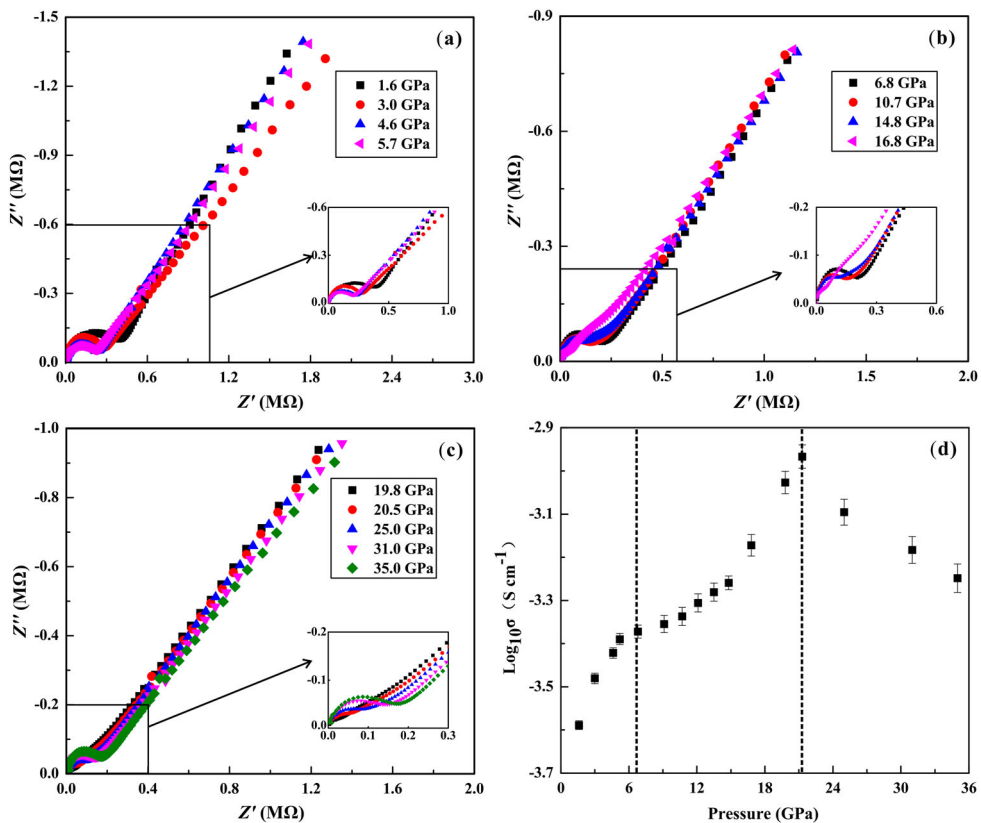


**Figure 4.** (a)–(c) Selected Nyquist plots of impedance spectra for goethite at different pressures. (d) Pressure-dependent electrical conductivity of goethite in the process of compression.

trend above 6.8 GPa. From 20.5 to 35.0 GPa, the electrical conductivity drastically decreases. Thus, three discrete pressure ranges can be identified by variation in the slope of pressure versus conductivity: from ambient pressure to 6.8 GPa, 6.8–20.5 GPa and 20.5–35.0 GPa. Although, opinion varies on the pressure-induced phase transition for goethite at room temperature. In light of our Raman and electrical conductivity measurements, the variation of conductivity and Raman modes for goethite at  $\sim 7$  and  $\sim 20$  GPa could be attributed to pressure-induced phase transitions.

To explore the evolution of electronic structure in goethite under high pressure, pressure dependence of the bulk relaxation frequency was shown in Figure 5. Electrical carrier transport in the grains of the sample can be described as a charging process in an R-CPE resonance circuit. Therefore, the relaxation frequency represents the charge–discharge rate of dipole oscillation, and its activation energy is the energy required to activate the resonance. The relaxation frequency under different pressures is in accord with the Arrhenius relationship as follows:

$$d(\ln f)/dP = -(1/k_B T)(dH/dP), \quad (2)$$

where  $T$  is room temperature,  $H$  is the activation energy, and  $k_B$  is the Boltzmann constant. The results of the pressure dependence of the activation energy are listed in Table 2, with errors of less than 2%. The gradient changes in the relaxation frequency ( $f$ ) of the sample in Figure 5 are consistent with the variations of electrical conductivity, and also indicate the phase transitions for goethite. Between 1.6 and 6.8 GPa, the negative value of  $dH/dP$  indicates that the required energy for carriers to participate into the conduction and to overcome the barrier in the relaxation process decrease with increasing pressure. And carrier density increases with the reduced activation energy, which will lead to the increased conductivity with pressure for goethite. At the pressure range of 6.8–20.5 GPa, the activation energy still decreases with the increasing pressure with a negative

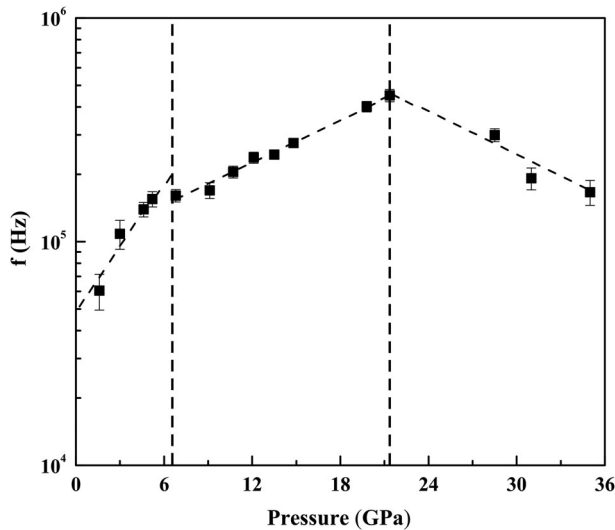


**Figure 5.** Pressure dependence of relaxation frequency of goethite. The dashed lines are linear fittings of the data.

**Table 2.** Pressure dependence of activation energy of goethite.

Pressure region (GPa)	dH/dP (meV GPa <sup>-1</sup> )	Error (%)
1.6–6.8	–5.95	1.62
6.8–20.5	–1.78	1.82
20.0–35.0	1.91	1.21

rate of  $-1.78 \text{ meV GPa}^{-1}$ . The obtained positive rate of  $1.91 \text{ meV GPa}^{-1}$  after 20.0 GPa proves that the pressure-induced transition could make the charge discharge processes more difficult. And the increased activation energy with pressure is the reason why the electrical conductivity of goethite decreases above 20.0 GPa.

## Conclusion

Raman spectroscopy and electrical conductivity experiments are conducted to study the phase transitions for goethite at high pressure up to 35.0 GPa using a DAC. These results were obtained on the basis of high pressure Raman spectroscopy, electrical conductivity measurements. On the basis of the noticeable changes in the Raman-active modes and the variations in the slope of the conductivity, two pressure-induced phase transitions were revealed at  $\sim 7.0$  and  $\sim 20.0$  GPa, respectively. And the variations of activation energy determined by pressure dependence of relaxation frequency of goethite were also demonstrated the phase transitions.

## Disclosure statement

No potential conflict of interest was reported by the authors.

## Funding

This research was financially supported by the Strategic Priority Research Program (B) of the Chinese Academy of Sciences [grant number XDB 18010401], Key Research Program of Frontier Sciences of CAS [grant number QYZDB-SSW-DQC009], '135' Program of the Institute of Geochemistry of CAS, Hundred Talents Program of CAS and National Science Foundation of China of China [grant numbers 41474078, 41774099 and 41772042].

## References

- [1] Cornell R, Schwertmann U. The iron oxides. Weinheim: Wiley-VCH; 2003, 15: 409–420.
- [2] Yang H, Lu R, Downs R, et al. Goethite,  $\alpha\text{-FeO}(\text{OH})$ , from single-crystal data. *Acta Crystallogr E*. 2006; 62: i250–i252.
- [3] Sakamaki T, Suzuki A, Ohtani E. Stability of hydrous melt at the base of the earth's upper mantle. *Nature*. 2006;439:192–194.
- [4] Pearson D, Brenker F, Nestola F, et al. Hydrous mantle transition zone indicated by Ringwoodite included within diamond. *Nature*. 2014;507:221–224.
- [5] Pekel J, Cottam A, Gorelick N, et al. High-resolution mapping of global surface water and its long-term changes. *Nature*. 2016;540:418–422.
- [6] Hallis L, Huss G, Nagashima K, et al. Evidence for primordial water in Earth's deep mantle. *Science*. 2015;350:795–797.

- [7] Williams Q, Guenther L. Pressure-induced changes in the bond and orientation of hydrogen in FeOOH-goethite. *Solid State Commun.* **1996**;100:105–109.
- [8] Nagai T, Kagi H, Yamanaka T. Variation of hydrogen bonded O...O distances in goethite at high pressure. *Am Mineral.* **2003**;88:1423–1427.
- [9] Gleason A, Jeanloz R, Kunz M. Pressure-temperature stability studies of FeOOH using X-ray diffraction. *Am Mineral.* **2008**;93:1882–1885.
- [10] Otte K, Pentcheva R, Schmahl W, et al. Pressure-induced structural and electronic transitions in FeOOH from first principles. *Phys Rev B.* **2009**;80:205116.
- [11] Xu W, Greenberg E, Gkh R, et al. Pressure-induced hydrogen bond symmetrization in iron oxyhydroxide. *Phys Rev Lett.* **2013**;111:175501.
- [12] Suzuki A. Thermal equation of state of goethite ( $\alpha$ -FeOOH). *High Pressure Res.* **2017**;37:193–199.
- [13] Li M, Gao C, Ma Y, et al. New diamond anvil cell system for in situ resistance measurement under extreme conditions. *Rev Sci Instrum.* **2006**;77:123902. doi:10.1063/1.2400669.
- [14] Zhuang Y, Dai L, Wu L, et al. Pressure-induced permanent metallization with reversible structural transition in molybdenum disulfide. *Appl Phys Lett.* **2017**;110:122103.
- [15] Dai L, Zhuang Y, Wu L, et al. Pressure-induced irreversible amorphization and metallization with a structural phase transition in arsenic telluride. *J Mater Chem C.* **2017**;5:12157–12162.
- [16] Dai L, Liu K, Wu L, et al. Pressure induced irreversible metallization accompanying the phase transitions in  $Sb_2S_3$ . *Phys Rev B.* **2018**;97:024103.
- [17] Liu K, Dai L, Wu L, et al. Migration of impurity level reflected in the electrical conductivity variation for natural pyrite at high temperature and high pressure. *Phys Chem Mineral.* **2018**;45:85–92.
- [18] Legodi M, de Waal D. The preparation of magnetite, goethite, hematite and maghemite of pigment quality from mill scale iron waste. *Dyes Pigments.* **2007**;74:161–168.
- [19] Kustova G, Burgina E, Sanykov V, et al. Vibrational spectroscopic investigation of the goethite thermal decomposition products. *Phys Chem Mineral.* **1991**;18:379–382.
- [20] Juan-Farfan R, Bayarjargal L, Winkle B, et al. Pressure dependence of the lattice dynamics of diasporite,  $\alpha$ -AlO(OH), from Raman spectroscopy and density functional perturbation theory. *Phys Chem Miner.* **2011**;38:693–700.
- [21] Grevel K, Burchard M, Fasshauer D, et al. Pressure-volume-temperature behavior of diasporite and corundum: an in situ X-ray diffraction study comparing different pressure media. *J Geophys Res-Solid Earth.* **2000**;105:27877–27887.
- [22] Wiethoff F, Grevel K, Marler B, et al. P-V-T behavior of FeO(OH) and MnO(OH). *Phys Chem Mineral.* **2017**;44:567–576.
- [23] Suzuki A. High-pressure X-ray diffraction study of epsilon-FeOOH. *Phys Chem Mineral.* **2010**;37:153–157.
- [24] Efthimiopoulos I, Kemichick J, Zhou X, et al. High-pressure studies of  $Bi_2S_3$ . *J Phys Chem A.* **2014**;118:1713–1720.
- [25] Zhao J, Yang L, Yu Z, et al. Structural phase transitions and metallized phenomena in arsenic telluride under high pressure. *Inorg Chem.* **2016**;55:3907–3914.